PHYSICAL REVIEW B **69**, 224419 (2004)

Magnetic coupling between Fe nanoislands induced by capping-layer magnetic polarization

E. Navarro,[1] Y. Huttel,[2,3] C. Clavero,[2] A. Cebollada,[2] and G. Armelles[2]
[1]*Sección Departamental de Física Aplicada 1, Facultad de Veterinaria, Universidad Complutense, Av. Puerta de Hierro s/n, 28040 Madrid, Spain*
[2]*Instituto de Microelectrónica de Madrid-IMM (CNM-CSIC), Isaac Newton 8 (PTM) Tres Cantos, Madrid 28760, Spain*
[3]*Instituto de Ciencia de Materiales de Madrid, (ICMM-CSIC), 28029 Cantoblanco, Madrid, Spain*
(Received 10 December 2003; revised manuscript received 26 March 2004; published 30 June 2004)

A study on the interislands interaction in granular Fe(110) thin films grown on c-sapphire as a function of the islands size and the capping layer induced magnetization is presented. Islands size (ranging from 10 to 50 nm in diameter) and physical contact between them can be monitored with the deposition time. While Al and MgO cappings do not modify the magnetic hysteresis loop of free islands surface, Pd and Pt give rise to a superparamagnetic-ferromagnetic transition in structures formed by small islands and a stronger interisland coupling in those formed by larger ferromagnetic islands. This improvement in the exchange interactions between islands is due to the induced magnetization of Pt and Pd localized at the interfaces between Pt-Fe(Pd-Fe) as evidenced by polar Kerr spectroscopy measurements and simulations.

DOI: 10.1103/PhysRevB.69.224419 PACS number(s): 75.75.+a, 75.70.Cn, 78.20.Ls, 75.50.Tt

I. INTRODUCTION

In order to design magnetic materials for specific applications, it is important to understand how their macroscopic properties arise from the interplay of microscopic parameters such as grain size,[1] intergrain coupling,[2,3] and anisotropies.[4,5] Furthermore, for the continuous increase of magnetic storage density,[6–8] it is crucial to know to what extent the independence of individual storage units can be maintained in the presence of intergrain coupling. The high fraction of atoms at the nanograins surface makes the nature of the interface critical in such a way that significant changes in behavior can be expected by changing the environment from that of a free particle to particles embedded in a matrix. In that sense, it is important to study the changes of the magnetic properties of nanoscale particles when they are coated with different type of materials: magnetic, nearly magnetic, and nonmagnetic.

It is well known that the magnetic properties of ultrathin continuous films can be tuned by deposition of adequate metal overlayers. The interplay between exchange interaction, (long range) dipolar interaction, and on-site magnetocrystalline anisotropy gives rise to a variety of magnetic phenomena with no counterpart in three-dimensional systems, such as perpendicular magnetic anisotropy[9–11] and magnetic reorientation transition.[12–14] The influence of various cover layers such as Au, Cu, Pd, and Ag on perpendicular magnetic anisotropy has been investigated in Co ultrathin films.[15,16] Kisilievski *et al.*[14] have recently reported a silver overlayer thickness-driven magnetic reorientation transition in Co ultrathin films. The thickness dependence of the reorientation transition in Fe(110) ultrathin films grown on W(110) can be tailored by controlled modification of the surface (anisotropy) of the Fe films through the deposition of noble metal (Ag and Au) ovelayers.[13] An in-plane to out-of-plane reorientation of magnetization upon the growth of an ultrathin Au cap layer on a slightly thicker Fe film has been reported recently by Zavaliche *et al.*[9]

On the other hand it is well documented that a nonmagnetic metal in contact with a ferromagnetic one often displays magnetic order.[17–19] In such systems, the interaction between the electronic states of the various elements and the 3*d* states of the ferromagnetic metal plays a fundamental role. Pd and Pt are on the border of being ferromagnetic and small perturbations may therefore lead to a spontaneous spin polarization. In particular, Pd-Fe (Pt-Fe) alloys have been extensively studied, with the conclusion that their magnetic properties depend on the mixing between Fe 3*d* majority band and Pd 4*d* (Pt 5*d*) states.[20] The same situation occurs in thin Pd (Pt) films grown on iron: spin-resolved photoemission studies have indeed shown a polarization effect in the first atomic layer in both Pd/Fe(001) (Ref. 18) and Pt/Fe(001),[19] indicating that the Fe 3*d*-Pd 4*d* (Pt 5*d*) interaction gives rise to a redistribution of interfacial states which induces a ferromagnetic coupling of the film with the substrate.

In this work we show that the induced magnetization of Pd and Pt can be used to drastically change the magnetic properties of a system formed by Fe nanoislands that shows a superparamagnetic or weakly ferromagnetic behavior depending on islands size. The magnetic properties of uncapped and capped nanoislands with different type of materials, are compared by combining *in situ* and *ex situ* techniques that makes possible to determine for example the influence of the capping layer in a much more direct way than if only *ex situ* techniques were used. Magneto-optical characterization shows that Pt as well as Pd are magnetic polarized, which in turn induces an enhancement of the magneto-optical effect in the technologically interesting (sensors or new generation recording media) energy range (short wavelengths) as observed in other Pt related systems like Pt/Co (Refs. 21 and 22) and Pd/Co (Ref. 23) multilayers.

II. EXPERIMENT

Fe was grown at 700 °C by triode sputtering (work pressure, $P_{Ar}=1.10^{-4}$ mbar, and deposition rate 0.4 nm/min) on c-sapphire substrates in a system with a base pressure in the

low 10^{-9} mbar range. In all cases, a 2.5 nm layer of capping material (Al, MgO, Pd, Pt, or Fe) was grown at room temperature, either by triode sputtering (Al, Pd, Pt, Fe) or laser ablation (MgO). We have previously observed the growth of (110) oriented Fe in an islanded fashion when deposited at elevated temperatures onto basal plane sapphire substrates,[24] where TEM measurements,[25] indicated that the (110) textured growth of Fe present three in-plane equivalent azimuthal orientations ($[1-10]Fe//\langle 11-20\rangle Al_2O_3$) as expected from the symmetry of the substrate.[24] The island size and morphology for different Fe deposition times were studied with atomic force microscopy (AFM). *In situ* magneto-optical transverse Kerr loops were performed on uncapped and capped Fe islands immediately after deposition keeping the samples in a base pressure in the low 10^{-9} mbar. Very low in-plane magnetic anisotropy was concluded by the identical loops obtained rotating the sample formed by Fe islands with respect to the magnetic field every 10°. Polar Kerr spectra were acquired *ex situ* with a maximum field of 1.5 T.

III. RESULTS AND DISCUSSION

A. AFM results: Morphology of the Fe islands

Ex situ AFM measurements performed in capped and uncapped samples yield very similar morphologies and island sizes which evidences the conformal nature of the capping materials. All the samples presented islands with rounded tops. Average islands size ranges from 10 nm in-plane diameter (d) and 1 nm height (h) up to 50 nm in-plane diameter and 7 nm height. Both, average d and h increase for longer deposition times. The AFM characterization of capped samples was performed two times; the first time immediately after the sample growth and the second time one month latter. Similar structural parameters were found in our case in contrast to other studies[26] that have reported a time-dependence of islands morphology. The morphology of three samples with 0.6, 1.6, and 2.4 nm nominal Fe thickness and covered with Pt is shown in Fig. 1. The nominal thickness corresponds to that of a continuous and flat Fe film, if grown on the same substrate but at lower temperature (giving rise to 2D growth). The topography images are displayed together with the diameter and height dispersion values in the form of d-histogram and h-histogram. The number of events represents the number of islands and pixels included in the scanned area in the case of d and h histogram, respectively. The average diameter and height as well as the standard deviations, σ_d and σ_h for d and h, respectively, are included in each plot. The samples with smaller islands (0.6 and 0.8 nm nominal Fe thickness) show a homogeneous size distribution as can be observed in d and h histograms in Fig. 1(a) for 0.6 nm nominal Fe thickness. By increasing the amount of deposited iron (1.6 and 2 nm nominal Fe thickness), the islands grow filling up completely the substrate. The lateral islands growth is limited by the presence of neighboring islands that coalesce for higher deposition times giving rise to a slightly inhomogeneous size distribution as can be seen in Fig. 1(b) for 1.6 nm nominal Fe thickness. The effect of the coalescence of islands in the size distribution is more evident in Fig. 1(c), where a wider distribution of islands size (d ranging from 10 to 55 nm and h ranging for 2 to 14 nm) is observed in the d and h-histograms, respectively. In this work we will study samples with Fe islands that display a narrow distribution of size. Therefore in the following we will focus our study on the properties of systems with Fe islands with $d \leqslant 18$ nm which corresponds to nominal Fe thickness $\leqslant 2$ nm.

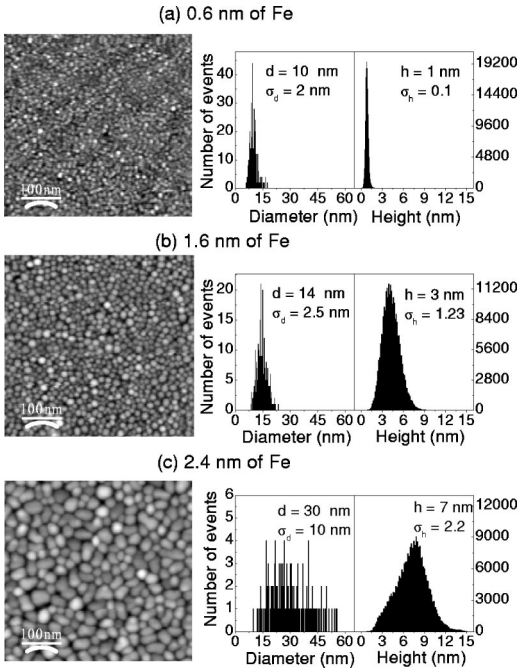

FIG. 1. AFM topography images and island diameter (d) and height (h) histograms with the calculated standard deviations, σ_d and σ_h for d and h, respectively, of samples with islands of different nominal Fe thickness: (a) 0.6 nm, (b) 1.6 nm, and (c) 2.4 nm. Average d, h, σ_d, and σ_h are included in each plot.

B. Uncapped and Pt capped Fe islands: Island size dependence

In Figs. 2(a)–2(h) we show a complete magnetic characterization for a series of uncoated and Pt-coated samples with different island sizes. In the left column [Figs. 2(a)–2(d)], the *in situ* transverse Kerr hysteresis loops for uncapped (open circles) and Pt capped (continuous line) Fe islands of different sizes are shown. In the right column of [Fig. 2(e)–2(h)], the corresponding polar Kerr loops for the same Pt capped islands are displayed.

For the uncapped islands there is a clear evolution of the loop's shape, starting from the absence of hysteresis (intensity linearly proportional to the applied magnetic field) for $d=10$ nm, with a weak MOKE, followed by the appearance of a loop with a gradual increase of coercive field and remanence for d equal to 12, 14, and 18 nm, even though saturation is not reached due to the limited maximum magnetic field available in the present *in situ* Kerr set-up.

In order to elucidate the magnetic behavior of uncapped Fe islands with $d=10$ nm, Al capped islands of identical size

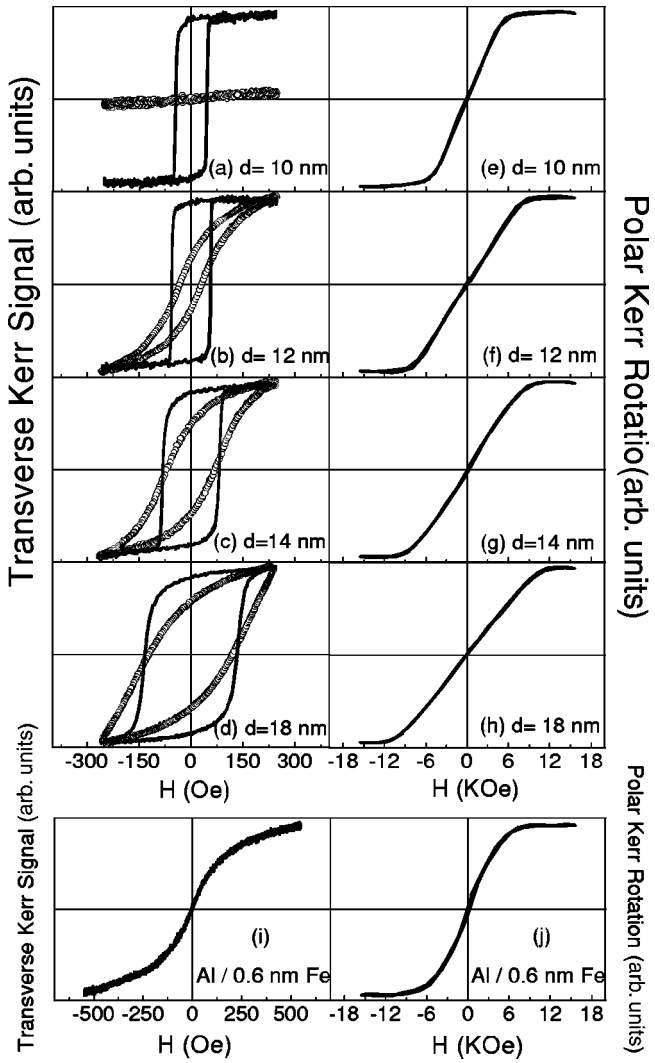

FIG. 2. *In situ* transverse Kerr loops (a) to (d) of a series of uncoated (–o–) and Pt-coated (–) Fe islands with different island sizes. From (e) to (h): *ex situ* polar Kerr loops for the Pt capped samples. (i) and (j): *ex situ* transverse and polar, respectively, Kerr loop of Al-covered Fe islands with 10 nm average diameter.

were measured ex situ with higher field in transverse and polar geometry [Figs. 2(i) and 2(j), respectively]. The obtained loops show an absence of remanence and coercivity as in the case of a superparamagnetic behavior. In addition, a complete study of the transverse susceptibility (χ_t) of samples presented in this work is being performed.[27] Preliminary results of the χ_t measured on Al covered 10 nm islands show a pronounced peak in $H=0$ which reaffirms the superparamagnetic behavior of the sample. In this case the uncapped Fe and Al-capped islands do not coalesce, being magnetically isolated from each other and small enough to be superparamagnetic at room temperature, which is consistent with their average volume. An increase of 2 nm in the islands diameter and 0.2 nm in height is enough to produce the appearance of a ferromagnetic hysteresis loop [Fig. 2(b)]. The observed remanence and coercivity in uncapped Fe islands with $d=12$ nm, indicate the presence of magnetic entities larger than for Fe islands with $d=10$ nm. Physical contact between islands (which increases with increasing deposition time until coalescence of individual islands) or a superparamagnetic-ferromagnetic transition inside the islands (as a consequence of new islands size), can be the origin of this ferromagnetic behavior. This is more evident for the samples with $d=14$ and 18 nm, where the uncapped samples exhibit hysteresis loops with higher remanence and coercivity.

The deposition of a Pt capping layer onto these structures drastically modifies the magnetization behavior of the islands. The Pt overlayer induces a magnetic connection between the Fe islands, giving rise to the sudden appearance of a clear square hysteresis loop, with a sharp reversal of the magnetization for the initially superparamagnetic 10 nm islands, indicating a collective switching of all islands magnetization. In the case of the islands that presented hysteresis in the uncapped situation ($d>10$ nm), the Pt layer induces a more squared loop due to a stronger magnetic interaction between islands. Coated samples with $d=12$ nm and $d=14$ nm exhibit a simultaneous magnetization reversal for most of the sample, i.e., the islands are strongly coupled [Figs. 2(b) and 2(c)]. Finally, the sample with $d=18$ nm [Fig. 2(d)] shows hysteresis loops where the magnetization reversal takes place at different switching fields, as a consequence of a wider size distribution of islands. In all cases, the deposition of Pt produces a stronger inter island magnetic coupling that leads to a superparamagnetic-ferromagnetic transition for d=10 nm and to stronger coupling for $d>10$ nm. This coupling effect produced by the Pt capping is probably due to the high magnetic polarizability of Pt (Ref. 28) that becomes slightly magnetic in contact with the Fe islands and acts as an exchange transmitter between them.

In Pt/Fe multilayers[29] or Pt films grown on Fe,[30] an induced Pt magnetic moment of $0.5\mu_B$/atom has been measured up to 5 atomic layers (about 1 nm) at the Pt/Fe interface. Taking this polarization depth as a reference, two islands laterally separated by approximately 2 nm could be magnetically connected through polarized Pt (each island would polarize 1 nm of Pt).

Additionally, as it can be seen in left column of Fig. 2, the coercive field in the transverse geometry gradually increases with islands size, which is consistent with a single domain nature of the islands, since multidomain nature appears beyond a critical size producing a reduction in Hc.[31,32] The evolution of the corresponding polar Kerr loops (right column of Figs. 2) shows a continuous increase of saturation field (Hs) due to the increasing island size, with the consequent increase in demagnetizing field as the island approach the thin film limit. The 3D nature of the islanded structures makes this limit (2.2 T) difficult to reach in practice, even for the largest diameters.

C. Influence of the capping layer nature

Once shown the strong modification induced by the Pt capping layer in the magnetization of nanometric Fe islands, and possibly due to the induced magnetization of Pt, we will confirm this effect by studying a series of samples, all of them with approximately the same island diameter (12 nm)

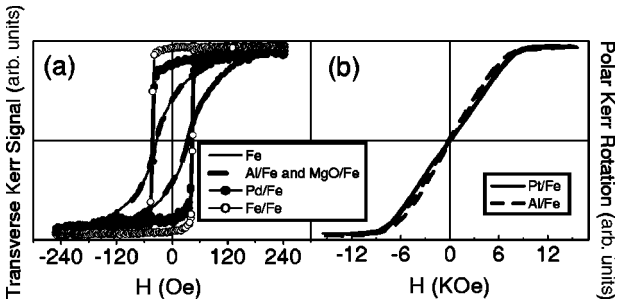

FIG. 3. (a) *In situ* transverse Kerr loops for uncapped Fe islands with 12 nm average diameter and covered with Al, MgO, Pd, and Fe capping layers grown at room temperature. (b) *Ex situ* polar Kerr loops for Pt and Al capped Fe islands with 12 nm average diameter.

and with cappings of different magnetic nature, magnetic-polarizable (Pd), nonpolarizable (Al and MgO), and ferromagnetic (Fe), all of them grown at room temperature.

In Fig. 3(a) we show the *in situ* transverse hysteresis loops of uncapped Fe islands with $d \approx 12$ nm and also capped with Al, MgO, Pd, and Fe. As can be seen, the loop obtained for the uncapped sample remains unaltered upon deposition of either Al or MgO, magnetically non-polarizable materials. Nevertheless, deposition of magnetically polarizable Pd and Pt [shown in Fig. 2(b)] leads to a more square loop, with higher remanence and sharp magnetization reversal. Finally, the use of a Fe capping layer produces a squared hysteresis loop with 100% remanence due to the obvious magnetic connection of the islands mediated by the ferromagnetic Fe overlayer. The similarity between the effects produced by Pt, Pd, and Fe confirms the magnetic nature of the capping as the main reason for this change. Despite this evidence, the effect could be alternatively explained by the presence of an out-of-plane magnetic anisotropy in the uncapped islands, that remains upon deposition of either Al or MgO cappings, but that disappears if the islands are covered with Pt, Pd, or Fe. For example, strain effects upon Pt and Pd deposition could modify the global anisotropy via magnetoelastic effects, or interfacial mixing between Fe and Pt (Pd) could locally produce high anisotropy FePt (Refs. 33 and 34) and FePd (Ref. 35) alloys. To answer this question we show in Fig. 3(b) the polar Kerr loops measured for 12 nm diameter islands covered with Al and Pt, representative cappings. As it can be observed, very similar hysteresis loops are obtained. A slightly different slope (13% larger for the Al capped sample) is observed between the two samples. This can be due to the increase in magnetic diameter of the Pt capped islands due to the polarization of the Pt surrounding them, with the subsequent increase of demagnetizing factor [see for comparison the evolution of slopes in Figs. 2(e)–2(h)] with respect to the Al capped islands, where the diameter of the magnetic entity remains the same. However, this slight change in slope seems to be too small to be attributed to significant changed of the magnetic anisotropy, since in addition remanence and coercivity are absent in both samples.

D. Magnetic polarization of Pt and Pd as confirmed by polar Kerr spectroscopy

As previously shown, we interpret the Pt (Pd) effect in free islands magnetic behavior as due to the magnetic polarization of these two materials which become weakly ferromagnetic at the interface with the Fe islands and transmit the exchange interaction between them. Therefore, islands that present superparamagnetic or weak ferromagnetic behavior would become magnetically connected through the Pt (Pd) magnetic polarized layer exhibiting a marked ferromagnetic character. In order to confirm this assumption we have measured and simulated the polar Kerr rotation spectra for the samples presented in this work and studied what should be the effect of the magnetic polarization of Pt and Pd in the rotation spectra. The magneto-optical characterization was carried out in a polar Kerr configuration in the spectral range 1.5–4.5 eV, the applied magnetic field being set to 1.5 T. Figure 4(a) shows the experimental rotation spectra for samples with different metallic materials covering the Fe islands with $d \approx 12$ nm. As can be observed despite the similar dielectric constants of Al, Fe, Pt, and Pd, the experimental spectra are very different. In particular, in the ultraviolet region the sign of the rotation for the Fe and Al capped samples is different from the Pt and Pd capped ones, while being the same in the visible-infrared region. We associate these differences to the magnetic polarization of Pt and Pd, and therefore to the appearance of an additional magneto-optical activity not present if they were not polarized.

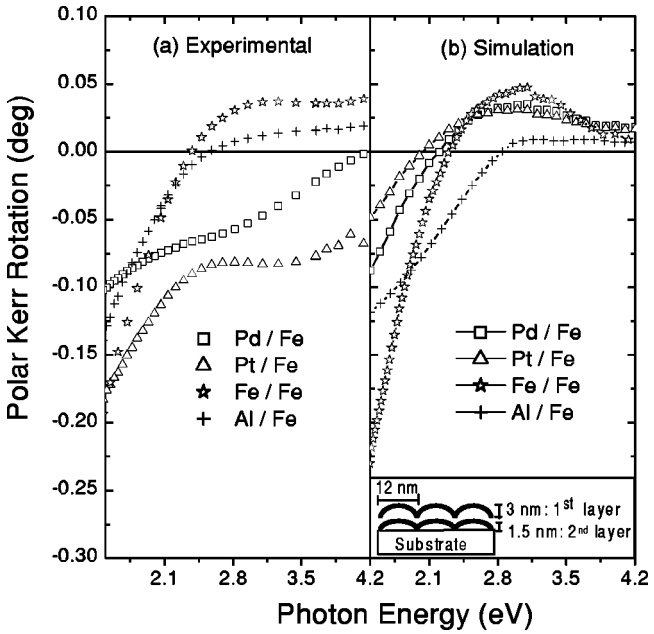

FIG. 4. (a) Experimental polar Kerr spectra for Fe islands with 12 nm average diameter covered with different capping materials: Pd, Pt, Fe, and Al. (b) Corresponding simulations. The inset shows the structure considered in the simulation.

This assumption is supported by the simulation of the Kerr rotation spectra of the films. The calculations were done using the structure shown in the inset of Fig. 4(b), where the different films are simulated as a two layer structure; the first layer is a rough capping layer, simulated as a 3 nm thick layer of a medium made of, Fe, Al, Pt, or Pd islands embedded in air. The second layer is a 1.5 nm thick layer of a medium made of Fe islands embedded in a Fe, Al, Pt, or Pd matrix, respectively. A transfer matrix formalism[36] has been

used to calculate the Kerr rotation spectra of the films, using for the substrate a refractive index of 1.75. The dielectric tensors of the layers were obtained from the dielectric tensor of the islands and the matrix, the shape and amount of islands using an effective medium approximation.[37] The diagonal components of the dielectric tensors of Fe, Al, Pd, and Pt were obtained from Ref. 38, the magneto-optical components of the dielectric tensor of Fe were obtained from Ref. 39, and the shape and amount of island were obtained from AFM results (disklike shape island with a filling factor of 50%). As can be seen in Figs. 4(a) and 4(b), there is a reasonable agreement in the shape, rotation values and signs, between experiment and simulation for Al/Fe and Fe/Fe cases, confirming the validity of the assumed structure and simulation formalism. On the contrary, if we consider that Pt and Pd in the two layers are not magnetic polarized the simulated spectra are similar to the Al or Fe case but different from the experimental results [see Figs. 4(a) and 4(b)]. Nevertheless, if Pt or Pd are magnetic polarized their magneto-optical constants should be different from zero. A rough idea of these magneto-optical constants could be obtained from the Kerr rotation and ellipticity of FePt (Ref. 40) (FePd) (Refs. 41 and 42) alloys by assuming that the 50% alloy is an effective medium composed of Pt (Pd) magnetic polarized particles (spheres) and Fe particles (spheres), as follows:

$$\varepsilon_{\mathrm{Pt}}^{xy} = \varepsilon_{\mathrm{FePt}}^{xy} + \frac{(\varepsilon_{\mathrm{FePt}}^{xy} - \varepsilon_{\mathrm{Fe}}^{xy})[\varepsilon_{\mathrm{FePt}}^{xx} + 0.33(\varepsilon_{\mathrm{Pt}}^{xx} - \varepsilon_{\mathrm{FePt}}^{xx})]^2}{[\varepsilon_{\mathrm{FePt}}^{xx} + 0.33(\varepsilon_{\mathrm{Fe}}^{xx} - \varepsilon_{\mathrm{FePt}}^{xx})]^2},$$

where $\varepsilon_{\mathrm{Pt}}^{xy}$ is the magneto-optical constant of Pt (or Pd), $\varepsilon_{\mathrm{Fe}}^{xy}$ is the magneto-optical constant of Fe, and $\varepsilon_{\mathrm{FePt}}^{xy}$ is the magneto-optical constant of FePt (or FePd) obtained from the Kerr rotation and ellipticity spectra. $\varepsilon_{\mathrm{Fe}}^{xx}$, $\varepsilon_{\mathrm{Pt}}^{xx}$, and $\varepsilon_{\mathrm{FePt}}^{xx}$ are the diagonal components of the dielectric tensor of Fe, Pt (or Pd), and FePt or (FePd), respectively.

In Figs. 5(a) and 5(b) we present the experimental and simulated Kerr rotation spectra for Fe particles with a Pt (Pd) capping having different degrees of magnetic polarization. Curve A corresponds to a simulation were Pt or Pd are not polarized (i.e., Pt or Pd in the two layers have magneto-optical constants equal to zero) and, as we have shown above, the calculated spectra are very different from the experimental ones. On the other hand, if the Fe particles are embedded in a Pt (Pd) magnetic polarized matrix and covered with no polarized Pt (Pd) (Pt+air, Pd+air) (i.e., Pt or Pd have magneto-optical constants different from cero in the second layer and equal to zero in the first layer), the simulated spectra (B) are more similar to the experimental case with qualitative and even quantitative agreement. Finally, if we assume that additionally the Pt (Pd) in the first layer (Pt+air, Pd+air) is polarized, the calculated rotations (simulation C) are negative in the whole spectral range, but too far from the experimental data.

We can therefore conclude that a polarized Pt (Pd) layer in the near region with the Fe, covered by an unpolarized Pt (Pd) layer is likely the picture closest to the actual structure. From those simulations, we can also estimate the amount of Pt (Pd) magnetic polarized which is about 0.7 nm of nominal thickness. This confirms that the strong variations in magnetic properties of Pt/Fe and Pd/Fe in comparison with those of free Fe islands or Al/Fe islands can be mainly attributed to the magnetic polarization of the Pt (Pd) layer in the Pt/Fe (Pd/Fe) interface region.

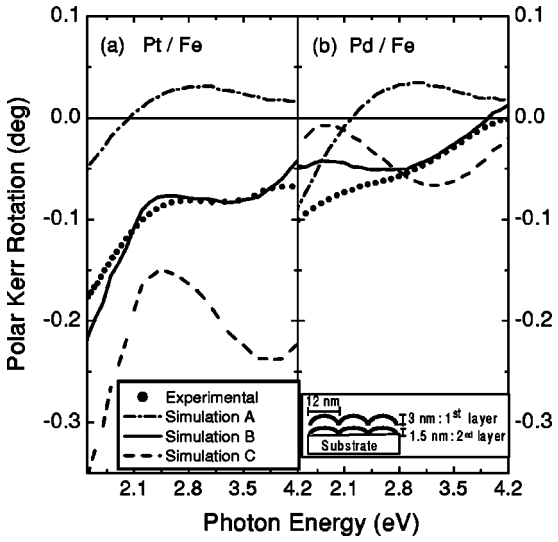

FIG. 5. (a) Pt/Fe system (b) Pd/Fe system. Experimental polar Kerr spectra together with three different simulations. Simulation A: Pt (Pd) is not polarized; Simulation B: only the Pt (Pd) in the second layer is polarized; Simulation C: Pt (Pd) is polarized in the two layers.

IV. CONCLUSIONS

To conclude, we have studied nanostructured systems formed by Fe islands with a clear dependence of morphology and size distribution of islands with the amount of deposited Fe: a homogeneous size and shape distribution of islands for small amounts of Fe and an increase of coalescence for larger amounts of Fe. The morphology of the Fe islands affects directly the magnetic properties that strongly depend on the size and on the interislands interaction: isolated islands (10 nm of diameter) exhibit superparamagnetic behavior while a ferromagnetic phase is developed when islands size increases to 12 nm. We have shown that the deposition of Pt (Pd) on top of very close to each other superparamagnetic Fe islands yields to a superparamagnetic to ferromagnetic transition suppressing their intrinsic superparamagnetic character. When the Fe islands have bigger sizes and interact weakly, the Pt (Pd) capping layer increases significantly the magnetic interisland interaction. Both effects are due to the magnetic polarization of the Pt (Pd) layer that has been evidenced by measured and simulated magneto-optical Kerr rotation spectra, demonstrating that this polarization is limited to the region near the Fe islands, the outer Pt (Pd) region remaining unpolarized. In the case of a nonpolarizable capping layer (Al or MgO), no change is observed between the magnetic properties of capped and uncapped Fe islands.

ACKNOWLEDGMENTS

This work has been partially financed by the Spanish Commission of Science and Technology, Comunidad Autónoma de Madrid, and the Spanish Ministerio de Ciencia y Tecnología. Y.H. acknowledges the Consejo Superior de Investigaciones Científicas (CSIC) and Ramón y Cajal program for financial support.

[1] J. L. Dormann, D. Fiorani, F. Giammaria, and F. Lucari, J. Appl. Phys. **69**, 5130 (1991).
[2] J. F. Löffler, H.-B. Benjamin Braun, and W. Wagner, Phys. Rev. Lett. **85**, 1990 (2000).
[3] J. T. Lau, A. Frolisch, R. Nietubyc, M. Reif, and W. Wurth, Phys. Rev. Lett. **89**, 057201 (2002).
[4] J. P. Chen, C. M. Sorensen, and K. J. Klabunde, Phys. Rev. B **51**, 11 527 (1995).
[5] K. Kang, Z. G. Zhang, C. Papusoi, and T. Suzuki, Appl. Phys. Lett. **82**, 3284 (2003).
[6] C. P. Luo, S. H. Liou, L. Gao, Y. Liu, and D. J. Sellmyer, Appl. Phys. Lett. **77**, 2225 (2000).
[7] S. Y. Chou, Proc. IEEE **85**, 652 (1997).
[8] S. Sun, C. B. Murray, D. Weller, L. Folks, and A. Moser, Science **287**, 1989 (2000).
[9] F. Zavaliche, W. Wulfhekel, M. Przybylski, S. Bodea, J. Grabowski, and J. Kirschner, J. Phys. D **36**, 779 (2003).
[10] T. Duden and E. Bauer, Phys. Rev. B **59**, 468 (1999).
[11] K. Hyomi, Y. Oka, U. Hiller, and C. M. Falco, Appl. Phys. Lett. **80**, 282 (2002).
[12] H. J. Elmers and U. Gradmann, Appl. Phys. A: Solids Surf. **A51**, 255 (1990).
[13] L.-G. Baek, H. G. Lee, H.-J. Kim, and E. Vescovo, Phys. Rev. B **67**, 075401 (2003).
[14] M. Kisielewski, A. Maziewski, M. Tekielak, A. Wawro, and L. T. Baczewski, Phys. Rev. Lett. **89**, 087203 (2002).
[15] B. N. Engel, M. H. Wiedmann, and C. M. Falco, J. Appl. Phys. **75**, 6401 (1994).
[16] P. Beauvillain, A. Bounouh, C. Chappert, R. Mégy, S. Ould-Mahfoud, J. P. Renard, and P. Veillet, J. Appl. Phys. **76**, 6078 (1994).
[17] W. Weber, D. A. Wesner, and G. Güntherodt, Phys. Rev. Lett. **66**, 942 (1991).
[18] O. Rader, C. Carbone, W. Clemens, E. Vescovo, S. Blügel, W. Eberhardt, and W. Gudat, Phys. Rev. B **45**, 13 823 (1992).
[19] M. Finazzi, L. Braicovich, Ch. Roth, F. U. Hillebrecht, H. B. Rose, and E. Kisker, Phys. Rev. B **50**, 14 671 (1994).
[20] J. F. van Acker, P. J. W. Weijs, J. C. Fuggle, K. Horn, H. Haak, and K. H. J. Buschow, Phys. Rev. B **43**, 8903 (1991).
[21] X. Gao, S. D. W. Thompson, and J. A. Woollam, Appl. Phys. Lett. **70**, 3203 (1997).
[22] A. Vernes, L. Szunyogh, and P. Weinberger, J. Appl. Phys. **69**, 7291 (2002).
[23] E. R. Moog, J. Zak, and S. D. Bader, J. Appl. Phys. **69**, 4559 (1991).
[24] J. L. Menéndez, G. Armelles, C. Quintana, and A. Cebollada, Surf. Sci. **482-485**, 1135 (2001).
[25] C. Quintana, J. L. Menéndez, Y. Huttel, M. Lancin, E. Navarro, and A. Cebollada, Thin Solid Films **434**, 228 (2003).
[26] P. Poulopoulos, P. J. Jensen, A. Ney, J. Lindner, and K. Baberschke, Phys. Rev. B **65**, 64 431 (2002).
[27] J. Fernandez Calleja *et al.* (unpublished).
[28] E. Navarro, Y. Huttel, C. Clavero, G. Armelles, and A. Cebollada, Appl. Phys. Lett. **84**, 2139 (2004).
[29] W. J. Antel, Jr., M. M. Schwickert, and Tao Lin, Phys. Rev. B **60**, 12 933 (1999).
[30] R. Bertaco and F. Ciccaci, Phys. Rev. B **57**, 96 (1998).
[31] B. D. Cullity, *Introduction to Magnetic Materials* (Addison–Wesley, Reading, 1972).
[32] J. Löffler, H. Braun, and W. Wagner, Phys. Rev. Lett. **85**, 1990 (2000).
[33] B. M. Lairson, M. R. Visokay, R. Sinclair, and B. M. Clemens, Appl. Phys. Lett. **62**, 639 (1993).
[34] A. Cebollada, D. Weller, J. Sticht, G. R. Harp, R. F. C. Farrow, R. F. Marks, R. Savoy, and J. C. Scott, Phys. Rev. B **50**, 3419 (1994).
[35] C. Boeglin, H. Bulou, J. Hommet, and X. Le Cann, Phys. Rev. B **60**, 4220 (1999).
[36] M. Schubert, Phys. Rev. B **53**, 4265 (1996).
[37] J. L. Menéndez, B. Bescós, G. Armelles, R. Serna, J. Gonzalo, R. Doole, A. K. Petford-Long, and M. I. Alonso, Phys. Rev. B **65**, 205413 (2002).
[38] J. H. Weaver, C. Krafka, D. W. Lynch, and E. E. Koch, Phys. Daten **18–1** (1981).
[39] K. H. J. Buschow, in *Ferromagnetic Materials*, edited by E. P. Wohlfarth and K. H. J. Buschow (Elsevier Science, Amsterdam, 1988).
[40] T. Sugimoto, T. Katayama, Y. Suzuki, T. Koide, T. Sidara, M. Yuri, A. Itoh, and K. Kawanishi, Phys. Rev. B **48**, 16 432 (1993).
[41] G. Armelles, D. Weller, B. Rellinghaus, P. Caro, A. Cebollada, and F. Briones, J. Appl. Phys. **82**, 9 (1997).
[42] M. Shubert, Phys. Rev. B **53**, 4265 (1996).